Clustered Organization of Neurons with Similar Extra-Receptive Field Properties in the Primary Visual Cortex

Haishan Yao[2] and Chao-Yi Li[1]
Institute of Neuroscience
Shanghai Institutes of Biological Sciences
Chinese Academy of Sciences
Shanghai 200031
China

Summary

The primary visual cortex is organized into clusters of cells having similar classical receptive field (CRF) properties. Nonclassical, extra-receptive fields (ERFs) can either inhibit or facilitate the response elicited by stimulation within the CRF. Here, we report that in the primary visual cortex of cat, neurons with similar inhibitory or facilitatory ERF properties are also grouped into clusters. These clusters are randomly distributed in all cortical layers, with no detectable relationship with orientation and ocular dominance columns. This functional organization of neurons with respect to ERF properties may allow an efficient processing of global visual information.

Introduction

In the primary visual cortex, neurons with similar ocular dominance and orientation specificity are clustered into columns (Hubel and Wiesel, 1977). Neurons are also grouped together according to various classical receptive field (CRF) properties, e.g., direction of movement (Payne et al., 1981; Shmuel and Grinvald, 1996; Weliky et al., 1996), spatial frequency (Tolhurst and Thompson, 1981; Tootell et al., 1981; Shoham et al., 1997), color (Tootell et al., 1988), response latency, and temporal frequency (DeAngelis et al., 1999). Such grouping suggests that clustering of cells with common response properties is a general rule of cortical organization. Recent studies have shown that description based on CRF may not be sufficient for understanding some aspects of visual processing involving contextual information. Visual inputs from fields beyond CRF—the extra-receptive field (ERF)—were found to inhibit or facilitate responses elicited by CRF stimulation (Blakemore and Tobin, 1972; Maffei and Fiorentini, 1976; Nelson and Frost, 1978; Allman et al., 1985; Gulyas et al., 1987; DeAngelis et al., 1994; Li and Li, 1994; Sengpiel et al., 1997; Kapadia et al., 1999; Walker et al., 2000; Jones et al., 2001). Most neurons in the primary visual cortex exhibit either an inhibitory or facilitatory ERF property in a contrast and context-dependent manner (Levitt and Lund, 1997; Polat et al., 1998; Kapadia et al., 1999; Sceniak et al., 1999; Gilbert and Wiesel, 1990; Li, 1996; Rossi et al., 2001). As the evidence for the importance of ERF accumulates and our concept of receptive field evolves, it is of interest to consider the cortical organization of neurons with respect to their ERF properties.

Since neurons with similar CRF properties are known to cluster together into columns or blobs, it is natural to inquire whether neurons with similar ERF properties also show clustered distribution in the cortex. In the present study, we examined the functional architecture of cortical neurons with respect to ERF properties by determining inhibitory and facilitatory ERF properties of neurons in all cortical layers systematically. We found that cortical neurons with similar ERF properties are clustered together, and these clusters are randomly distributed within the cortex in a manner that is neither columnar nor laminar. Thus, the cortical organization with respect to ERF appears to obey the basic rule in cortical organization found for CRF; namely, the visual space is continuously represented by clusters of neurons of similar receptive field properties. Moreover, such clustered organization suggests a potential relationship between CRF and ERF architecture and is consistent with the continuity and completeness constraints proposed for the development of visual cortical maps (Hubel and Wiesel, 1977; Swindale et al., 2000).

Results

Identification of ERF Properties of Cortical Neurons

To determine the ERF properties of cells in the primary visual cortex of the cat, we used visual stimuli of sinusoidal gratings that drift at the optimal spatiotemporal frequency for the neuron. We first located the center of the CRF by moving rectangular grating patches along the axes perpendicular or parallel to the optimal orientation of the cell, and the peak of the response profiles for both axes was defined as the center of the CRF. We then measured the CRF diameter by performing an occlusion test, in which a mask of circular blank patch, concentric with the CRF, was gradually increased in size on the background of a full-field drifting grating (Figures 1A and 1B). The size of the mask at which the neuronal response decreased to the spontaneous level was defined as the diameter of CRF. The ERF property of the neuron was assessed by the neuronal response to the circular drifting gratings of different diameters (Figures 1C and 1D), which defines a "spatial summation" curve that reflects the influence of the surrounding area on the CRF response. We identified two classes of ERFs based on the shape of the spatial summation curve. The major class is the inhibitory ERF depicted by the example shown in Figure 1C. Maximum neuronal response was found for stimuli with a diameter corresponding to that of the CRF (dashed line, Figures 1A and 1C), and the response decreased with increasing grating size beyond the CRF. The minor class is the facilitatory ERF, which showed increasing neuronal response as the stimulus size increased beyond the CRF, with no sign of inhibition for stimulus diameter up to about 4-fold of the size of CRF (see Figure 1D).

[1]Correspondence: cyli@ion.ac.cn
[2]Present address: Department of Molecular and Cell Biology, University of California, Berkeley, California 94720.
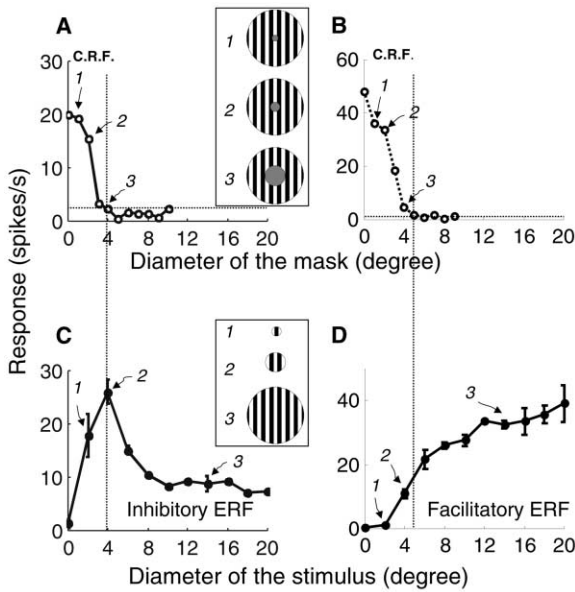
Figure 1. Determination of the CRF Size and ERF Properties

(A and B) Examples of the measurement of the CRF diameter. Blank patches of different diameters were presented randomly on the background of a full-field grating to concentrically occlude the CRF. Each arrow points to a certain mask diameter, which is shown in the inset. The mask diameter at which the response was reduced to the spontaneous level (horizontal dotted lines) is defined as the size of CRF (dotted vertical lines).

(C) An example of spatial summation curve of a neuron with inhibitory ERF. The neuron reached maximum response at CRF stimulation (vertical dotted line) and showed decreasing response to stimuli of increasing diameter beyond CRF. Arrows point to stimulus diameters corresponding to those shown in the inset.

(D) An example of spatial summation curve for a neuron with facilitatory ERF. The response increased progressively with increasing stimulus size both within and beyond the boundary of CRF (dotted line).

To quantitatively estimate ERF properties of the cortical neurons, we defined a summation index (S) by $S = (R_{ff} - R_{crf})/R_{crf}$, where R_{ff} and R_{crf} represent the response amplitude under full-field (set at 20°) and CRF stimulation, respectively. For neurons with inhibitory ERF, S is less than 0. For facilitatory ERF, S is greater than 0. Out of a total of 629 cells recorded in the present study, 358 cells (56.9%) showed inhibitory summation, and 271 cells (43.1%) showed facilitatory summation (Figure 2). In 448 (71.2%) of the overall population, we found a significant difference in R_{ff} and R_{crf} ($p < 0.05$, t test). Among these significant units, 278 cells showed inhibitory (dark blue bars in Figure 2) and 170 cells showed facilitatory (red bars in Figure 2) summation, with no significant difference in S value distribution between simple and complex cells ($p > 0.05$, Kolmogorov-Smirnov test).

Cortical Distribution of Neurons with Different ERF Properties

To map the distribution of neurons with different ERF properties in the primary visual cortex, we determined the ERF property of all neurons recorded by electrode penetration at different angles with respect to the cortical surface. Figure 3 shows samples of results from five different penetrations. The summation indices of all neurons recorded were shown (Figure 3, left panels), together with histological reconstruction of the electrode track through the cortical layers (Figure 3, right panels). Regardless of whether the penetration was tangential, oblique, or normal to the cortical surface, two general characteristics of the neuronal distribution were observed. First, we found that adjacent neurons along the electrode track tended to have similar ERF properties, either inhibitory ($S < 0$) or facilitatory ($S > 0$). Second, the length of electrode track covering neurons of similar ERF properties appeared to be limited, with each electrode track encountering several groups of neurons that alternated between inhibitory and facilitatory ERF properties. In total, twenty electrode penetrations were performed, among which six were relatively normal to the cortical surface (see Figures 3D and 3E). In these normal penetrations, the distribution of neuron groups with alternating inhibitory and facilitatory ERF properties was also found. This suggests that, unlike that for orientation and ocular dominance properties, cortical organization of neurons with respect to ERF properties is not columnar in the traditional sense; i.e., the response property is not conserved within a cortical column throughout all layers.

The clustering of neurons with different ERF was further demonstrated quantitatively by measuring the absolute difference in S ($|\Delta S|$) between any two recorded cells as a function of their distance along the electrode track, an analysis similar to that used previously (LeVay and Voigt, 1988; DeAngelis and Newsome, 1999; Born, 2000). For simplicity, we set the value 1 to all S values larger than 1. If there is cluster organization for neurons with respect to ERF properties, $|\Delta S|$ should be smaller for nearby cells than for distant cells. As shown in Figure 4A, we found that for both oblique and normal penetrations, the average $|\Delta S|$ increased with distance between the two cells and was significantly different from the grand average value of $|\Delta S|$ obtained from random sampling of cell pairs for 10,000 times ($p < 0.001$, one-way ANOVA). This result suggests that there exists a cluster organization for neurons with respect to ERF properties, resulting in similar S values for adjacent cells. To further examine the statistical significance of this phenomenon, we performed a two-way ANOVA test. The dependence on cell distance was significant ($p < 0.001$), whereas the difference in $|\Delta S|$ values between oblique and normal penetrations was less significant ($p = 0.03$). The latter difference may result from a few normal penetrations that happened to encounter larger clusters than did oblique penetrations, although the distribution of cluster length between oblique and normal penetrations was not significantly different ($p > 0.05$, Kolmogorov-Smirnov test). This analysis indicates that there is significant clustering of neurons with respect to ERF properties. Furthermore, the gradual increase in $|\Delta S|$ with distance found for normal penetrations suggests that such clustering is not organized in a columnar manner.

Laminar Distribution of Neurons with Different ERF Properties

To further study the cortical organization of neurons with respect to ERF properties, we examined the laminar
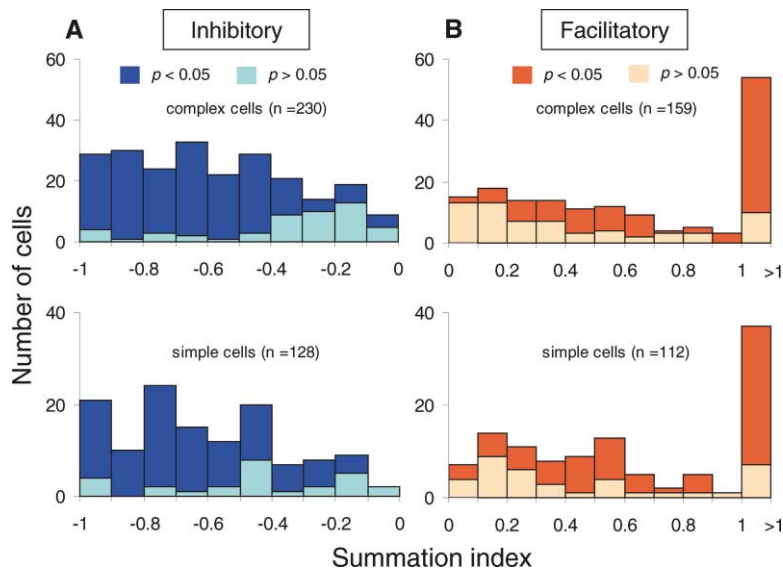
Figure 2. Distribution of Summation Index for Neurons with Inhibitory or Facilitatory ERF

Cells that showed a significant difference in R_{ff} and R_{crf} are indicated with dark blue ([A], inhibitory) and red ([B], facilitatory) bars, with no significant difference between the distribution of summation index (S) values for simple cells and complex cells (p > 0.05, Kolmogorov-Smirnov test). Among those significant units, S value for complex and simple cells with inhibitory ERF were -0.64 ± 0.02 and -0.65 ± 0.02 ($\pm$SEM), respectively; those for neurons with facilitatory ERF were 1.55 ± 0.19 and 1.33 ± 0.23 ($\pm$SEM), respectively.

distribution of these neurons. As shown in Figure 3, the changes in the ERF property did not appear to coincide with the crossing of boundaries of cortical layer, suggesting that neurons are not organized in accordance to their laminar location. We then determined whether neurons of inhibitory or facilitatory ERF property preferentially distribute in certain cortical layers. Figure 4B₁ shows the laminar distribution of all recorded neurons. We found that there were more neurons with inhibitory ERF in layer 2/3 and layer 4 than in the deeper layers, and more neurons with facilitatory ERF in layer 2/3 and layer 6 than in the middle layers. Such seemingly different laminar distribution, however, might be partly due to the difference of electrode track lengths that traversed different cortical layers. We have thus calculated the number of neurons per 1 mm length of electrode track for both types of cells in each cortical layer (Figure 4B₂). We found that after such normalization, neurons with inhibitory ERF were distributed approximately equally among cortical layers (p > 0.05, ANOVA), with an average of 6.6 neurons encountered per 1 mm length. For neurons with facilitatory ERF, some penetrations had more neurons in layer 6 than in layer 5. However, when the distributions from all penetrations were averaged, no statistically significant difference was found among all layers (p > 0.05, ANOVA), with an average of 4.5 neurons encountered per 1 mm electrode track. Thus, the organization of neurons with respect to ERF properties exhibits no cortical layer specificity.

The Shape and Size of Neuron Clusters
The above results suggest that neurons of the same ERF property tend to aggregate in clusters, and such clusters are not arranged in either a columnar or laminar manner. To further determine the dimension of these clusters, we calculated the cluster length over a range of penetration angles from 0° to 90° (Figure 4C). We define a cluster as the ensemble of neurons with the same ERF property (either $S > 0$ or $S < 0$) recorded consecutively. Cluster length was calculated as the difference of penetration distance between the first neu-

rons in two consecutive clusters. For this analysis, the length of the last cluster in each penetration was discarded. We found that, for clusters of either inhibitory or facilitatory ERF, there was no significant difference in cluster length among different penetration angles (p > 0.05, ANOVA). This suggests that both inhibitory and facilitatory clusters are isotropic in shape. Further analysis showed that the mean cluster lengths for neurons of inhibitory ERF and facilitatory ERF were 343 ± 41 μm and 254 ± 29 μm, respectively, with no significant difference in the distribution of cluster lengths between the two types (p > 0.05, Kolmogorov-Smirnov test; Figure 4D). Taken together, these results suggest that clusters of neurons of the same ERF property are roughly isotropic in shape and are similar in size for different types of clusters.

Relationship with Orientation and Ocular Dominance Columns
To examine the relationship between the clustered organization with respect to ERF properties and the conventional columnar organization in the cortex, we analyzed the orientation and ocular dominance properties of the recorded neurons. In the first analysis, we compared the degree of clustering for ERF properties with that for orientation and ocular dominance. The clustering of orientation selectivity was measured by a method described earlier (LeVay and Voigt, 1988; DeAngelis and Newsome, 1999; Born, 2000). We plotted the difference in optimal orientation between two cells (|Δorientation|) as a function of their distance along the electrode track, together with |ΔS| as a function of distance (Figure 5A). Both |Δorientation| and |ΔS| were significantly lower at short distances and approached the grand average value expected from random pairing at 300–400 μm (p < 5×10^{-15} for orientation, p < 2×10^{-8} for ERF property, ANOVA). We also analyzed the clustering of eye dominance from ten penetrations for which complete recordings of eye dominance were made. The probability of two cells showing the same eye dominance dropped to the chance level as their separation increased to >250
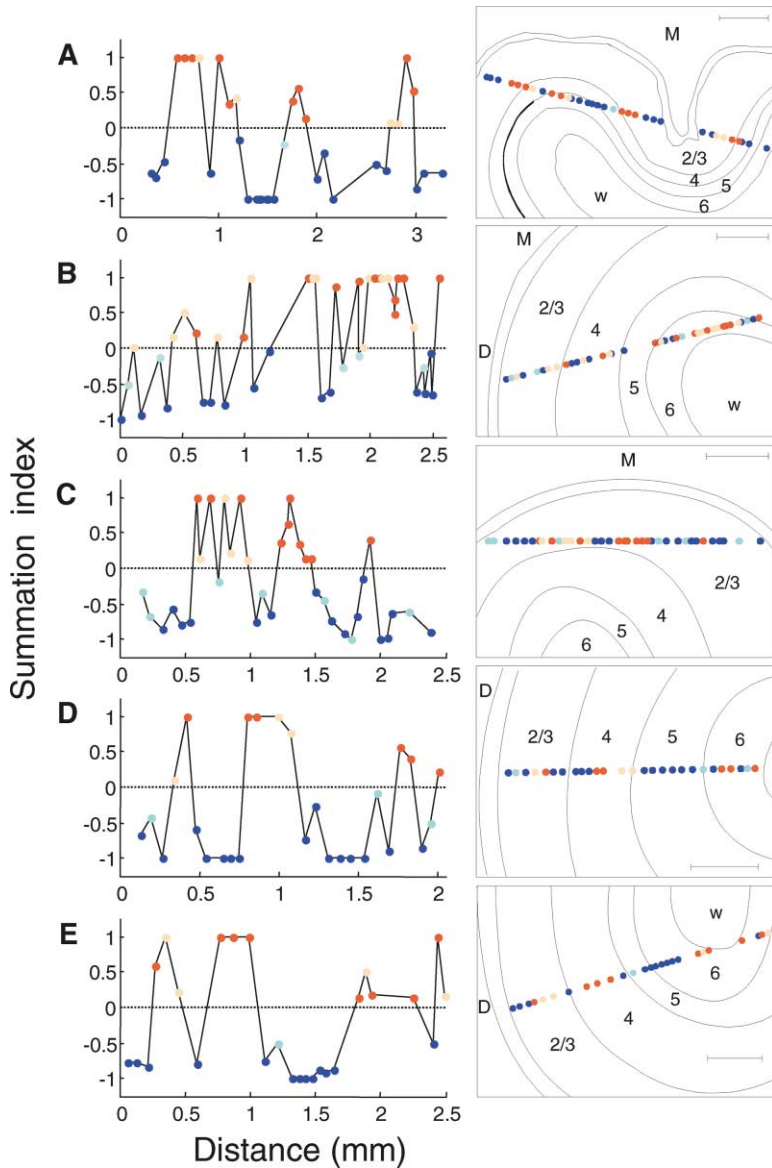
Figure 3. Cortical Distribution of Neurons with Different ERF Properties

Summation indices of all neurons recorded during electrode penetration of different angles through the cortex are shown on the left, with reconstructions of the corresponding electrode track on the right. Scale = 500 μm. Dark blue (p < 0.05, as in Figure 2) and light blue (p > 0.05) dots represent neurons with inhibitory ERF; red (p < 0.05) and orange (p > 0.05) dots represent neurons with facilitatory ERF. D, dorsal; M, medial; W, white matter.

μm (Figure 5B). Taken together, these results indicate that the degree of clustering for ERF property is similar to that for orientation selectivity and eye dominance, in that nearby neurons tend to have similar properties.

In the second analysis, we further examined the conventional CRF property of neurons within and across ERF clusters. For the relationship between ERF clusters and orientation columns, we calculated the difference of optimal orientation between two neighboring cells. As shown in Figure 5C (left panel), the distribution of orientation difference for neighboring cells of the same ERF properties, which reflects changes in orientation preference within the ERF clusters, is highly skewed in favor of small differences, with 65% of the pairs having an orientation shift of less than 40°. This distribution was not significantly different from that found for neighboring cells of the opposite ERF properties, which reflects changes in orientation preference across the boundary

of ERF clusters (Figure 5C, right panel) (p > 0.05, Kolmogorov-Smirnov test). Such a small shift of orientation preference observed within and across the clusters is consistent with the known organization of orientation columns in the primary visual cortex. When the relationship between ERF clusters and ocular dominance column was analyzed, we noted that the change in ocular dominance did not coincide with any drastic change in the ERF property. Cells within the same ERF clusters often shifted their ocular dominance between ipsi- and contralateral eyes. Furthermore, when the percentages of cells within each cluster (clusters that contain more than two cells) showing ipsilateral dominance were calculated, we found that a large number of clusters exhibit percentages that represent no clear ocular preference (Figure 5D). This suggests that the distribution of ERF clusters is independent of the boundary of the ocular dominance column. Finally, the mean number of neu-
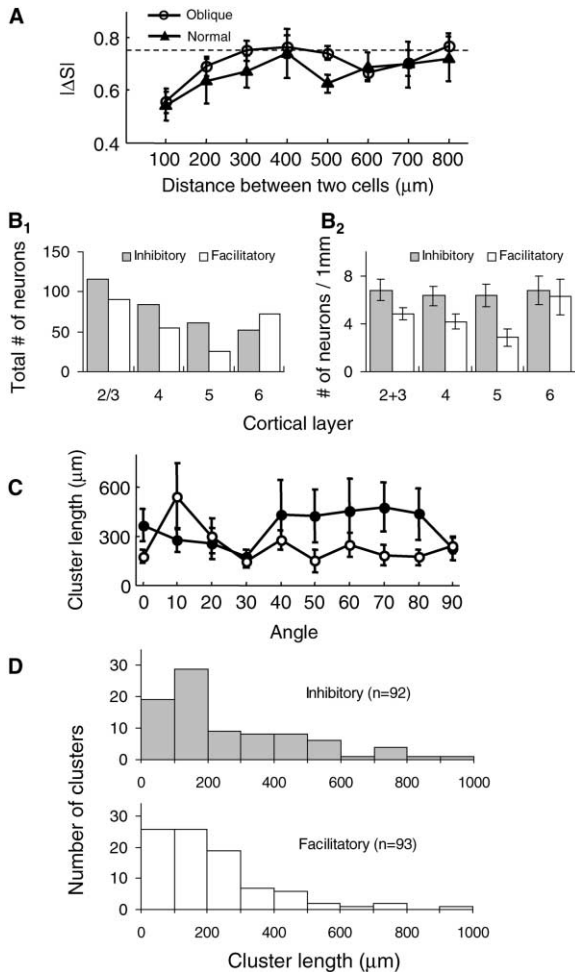
Figure 4. Analyses of Clustered Distribution

(A) Difference in S ($\pm$SEM, n = 180–580) between two cells as a function of distance along the electrode track. Circles and closed triangles indicate oblique and normal penetrations, respectively. The horizontal dashed line is the grand average $|\Delta S|$ expected from random pairing (n = 10,000). Penetrations 30°–90° away from cortical surface normal were classified as oblique penetrations; those <15° away from cortical surface normal were classified as normal penetrations.

(B) Laminar distribution of neurons with inhibitory (gray columns) or facilitatory (open columns) ERF. (B$_1$) The distribution of the total number of neurons in each cortical layer. (B$_2$) Same data set as (B$_1$); the number of neurons ($\pm$SEM, n = 11–18) is normalized by the electrode track length.

(C) Distribution of the cluster length ($\pm$SEM, n = 4–19) for clusters of different penetrating angles with respect to cortical surface. Closed and open circles represent inhibitory and facilitatory clusters, respectively.

(D) Cluster length distribution for clusters of neurons with inhibitory (gray columns) or facilitatory (open columns) ERF.
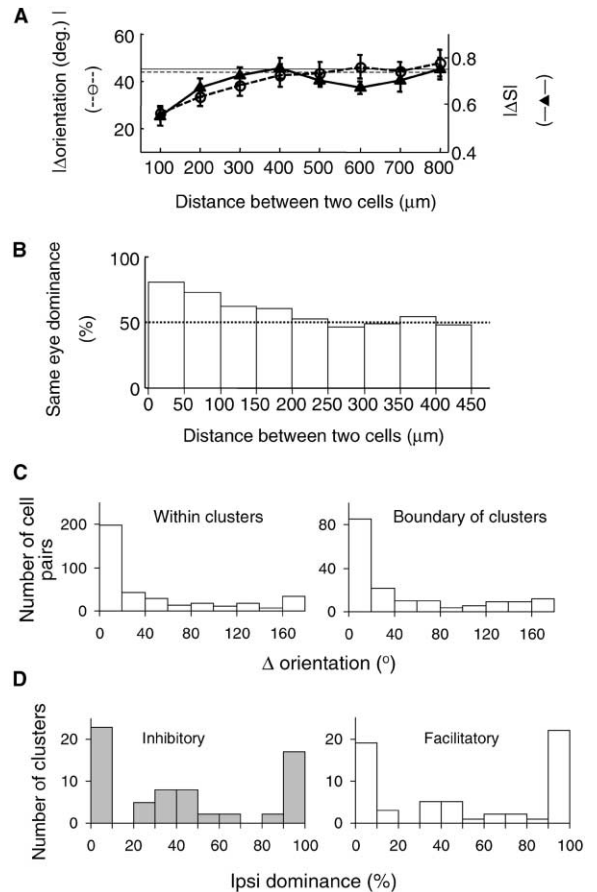

Figure 5. Relationship of ERF Clusters with Orientation and Ocular Dominance Columns

(A) Quantitative analysis of the degree of clustering for orientation selectivity and ERF properties. Circles and closed triangles show the difference in optimal orientation and S between two cells, respectively, as a function of distance along the electrode track ($\pm$SEM, n = 20). Horizontal dashed and solid lines indicate the average $|\Delta\text{orientation}|$ and $|\Delta S|$ expected from random pairing, respectively.

(B) Analysis of the degree of clustering for eye dominance. The probability of two cells having the same eye dominance as a function of distance was plotted. Horizontal dashed line indicates the probability that would be expected by chance.

(C) Distribution of the orientation difference between two neighboring cells within the ERF cluster (left) and that between two neighboring cells at the boundary of the cluster (right).

(D) Distribution of percentage of neurons with ipsilateral eye dominance among inhibitory ERF clusters (left) and facilitatory ERF clusters (right).

rons with ipsi- and contralateral dominance was not significantly different in either inhibitory or facilitatory ERF clusters (p > 0.05, Wilcoxon rank sum test), suggesting that the average numbers of inhibitory and facilitatory ERF clusters are roughly equal in the two ocular dominance columns. Taken together, these analyses support a model of randomly distributed clusters of neu-rons with similar ERF properties, with no detectable relationship with conventional functional architecture.

Discussion

Systematic examination of ERF properties of neurons in the primary visual cortex of the cat has led to our finding of the clustered organization of neurons with similar ERF properties. Neighboring neurons tend to exhibit similar ERF properties and are organized into clusters of either inhibitory or facilitatory ERF. Furthermore,

these clusters appear to be randomly distributed in all layers of the primary visual cortex. We found no organizational relationship between the ERF clusters and conventional orientation and ocular dominance columns. These conclusions are based on single-cell recordings of inhibitory or facilitatory effects of ERF stimulation. It is possible that other methods of assaying ERF properties may reveal additional aspects of neuronal organization that relate ERF clusters with CRF functional architecture.

Axon collaterals of cortical pyramidal neurons, which make long-range horizontal connections and allow integration of visual information over a wide cortical area, are known to be the underlying mechanism for spatial summation of inputs from the extra-receptive field (Gilbert, 1992). Anatomical studies indicate that axonal arbors associated with these long-range connections tend to form separate patches 200–300 μm in diameter (Amir et al., 1993), which can cross freely through diverse functional domains (Rockland and Lund, 1983; Malach et al., 1993). These clusters of axonal arbors may provide an anatomical basis for the observed ERF clusters, within which neurons are similarly influenced by arbors of the same axon that conveys visual information over the extended cortical area. In addition to the long-range horizontal connections, local inhibitory interneurons is also likely to contribute to the formation of inhibitory ERF clusters (McGuire et al., 1991; Das and Gilbert, 1999). Finally, feedforward inputs from LGN or feedback projections from higher cortical areas may also contribute to the formation of both facilitatory and inhibitory ERF clusters.

Previous studies have shown that the primary visual cortex contains orderly arranged cortical modules, each consisting of a complete set of ocular dominance and orientation columns and responsible for processing the information from a small part of the visual field (Hubel and Wiesel, 1977; Payne et al., 1981; Tolhurst and Thompson, 1981; Tootell et al., 1981, 1988; Shmuel and Grinvald, 1996; Weliky et al., 1996; Shoham et al., 1997; DeAngelis et al., 1999). However, visual stimuli are imbedded in complex scenes in which neighboring spatial locations are correlated in intensity and spatial frequency. Integration of the information beyond the local receptive field is critical for visual perception (Gilbert and Wiesel, 1990; Li et al., 1999). Information received by ERF can modulate the neuronal response of CRF stimulation, thus conveying the context where the stimulus is presented (Gilbert, 1998). Contextual stimuli of different texture features (orientation, spatial frequency, and speed and direction of movement) can activate cells with inhibitory ERF, whereas those of similar features can maximally excite neurons with facilitatory ERF (Li, 1996). In this sense, the inhibitory ERF may function as heterogeneity detectors, and the facilitatory ERF as homogeneity detectors. The present results provide further insights into the neuronal organization with respect to the ERF properties that are relevant for the global integration of visual information. The observed random clusters embedded throughout all cortical layers may provide several advantages. First, it ensures that global integration takes place at all parts of the visual field in the early stages of visual cortical processing. Second, ERF clustering in the primary visual cortex may help the

segregation of neuronal organization for local and global processing in higher visual areas (Born and Tootell, 1992). Third, clustering of neurons of similar ERF properties may help to increase the efficiency of information processing by minimizing the length of axons required for long-range integration, while satisfying the constraints of continuity and completeness in the development of the visual cortical map (Hubel and Wiesel, 1977; Swindale et al., 2000).

Experimental Procedures

Surgery
Preparations were identical to those described in detail in a previous paper (Li and Li, 1994). Briefly, cats were anesthetized prior to surgery with an i.m. injection of Ketanest (30 mg/kg). During recording, anesthesia was maintained with Flaxedil (10 mg/kg/h), d-tubocurarine chloride (0.25 mg/kg/h), urethane (20 mg/kg/h), and glucose (200 mg/kg/h) in Ringer's solution (1.5 ml/kg/h). ECG, EEG, end-expiratory CO_2, and rectal temperature were monitored continuously. The nictitating membranes were retracted and pupils dilated. Artificial pupils of 3 mm diameter were used. Contact lenses were applied to focus the retina onto a screen.

Visual Stimulation and Recording
Visual stimuli (sine wave gratings: contrast, 30%; luminance, 8.3 cd/m^2) were generated with an image synthesizer (Picasso, Innisfree, Cambridge, MA) and displayed on a CRT screen (Tektronix 608) subtended 20° × 20° (viewed at 28.5 cm). Recordings were made with fine-tipped (1–1.5 μm in diameter, 5–10 μm long) tungsten-in-glass microelectrodes (Li et al., 1995), which had an impedance of 10–30 MΩ and allowed high-resolution spatial sampling (50–100 μm) in our recording. Spikes were isolated with a lab-made two-level window discriminator. The shape of signal waveform, spontaneous activity, response amplitude, orientation selectivity, and receptive field location of each recording were carefully compared with those of the previously recorded neuron. We considered a unit to be the same as the previous one if all of the above parameters were the same. A neural signal with more than one parameter different from those of previously recorded signals was considered to be a new unit. Single units were isolated whenever possible. In about 10% of the recordings where a single unit could not be isolated, multiunit activity was recorded. Results from both types were combined. In 45 out of 55 sites where we recorded 2–3 single units simultaneously, all units in the same site had the same ERF property. Thus we considered most multiunits to be homogeneous in ERF properties.

All measurements were made during stimulation of the dominant eye. Each recording was first briefly characterized with drifting gratings. Gratings with optimal orientation, drifting direction, and spatial and temporal frequency were used for subsequent measurements. To locate the center of CRF, a rectangular grating patch was moved at successive positions along axes perpendicular or parallel to the optimal orientation of the cell. The peak on the response profiles indicated the center of CRF. The size of CRF was determined by an occlusion test in which the whole screen was filled with optimal drifting grating while the CRF was occluded by a concentric blank patch with variable diameters. The minimum diameter of the patch, which just reduced the firing of the cell to spontaneous level, is defined as the size of CRF. The nature of ERF was assessed from the spatial summation curve, which is the response to a set of randomly presented circular gratings of different diameter (from 0° to 20°). Response to each diameter was averaged for 10–20 cycles of the drifting grating, and standard errors were calculated for 3–6 repetitions.

Histological Reconstruction of the Electrode Tracks
At the end of each penetration, an electrolytic lesion was made by passing a current (10–15 μA for 10 s) through the tip of the electrode; then the electrode was withdrawn and two more lesions were made. At the end of the experiment, the animal was given an overdose of barbiturate and was perfused transcardially with 10% formaldehyde in 0.9% saline. The fixed brain was cut in blocks and sectioned to

80 μm thickness. Electrode tracks were reconstructed from the sections stained with cresyl violet. Cortical laminae were identified by the criteria of Gilbert (1977) and Lund et al. (1979).

References

Allman, J., Miezin, F., and McGuinness, E. (1985). Stimulus specific responses from beyond the classical receptive field: neurophysiological mechanisms for local-global comparisons in visual neurons. Annu. Rev. Neurosci. 8, 407–430.

Amir, Y., Harel, M., and Malach, R. (1993). Cortical hierarchy reflected in the organization of intrinsic connections in macaque monkey visual cortex. J. Comp. Neurol. 334, 19–46.

Blakemore, C., and Tobin, E.A. (1972). Lateral inhibition between orientation detectors in the cat's visual cortex. Exp. Brain Res. 15, 439–440.

Born, R.T. (2000). Center-surround interactions in the middle temporal visual area of the owl monkey. J. Neurophysiol. 84, 2658–2669.

Born, R.T., and Tootell, R.B. (1992). Segregation of global and local motion processing in primate middle temporal visual area. Nature 357, 497–499.

Das, A., and Gilbert, C.D. (1999). Topography of contextual modulations mediated by short-range interactions in primary visual cortex. Nature 399, 655–661.

DeAngelis, G.C., and Newsome, W.T. (1999). Organization of disparity-selective neurons in macaque area MT. J. Neurosci. 19, 1398–1415.

DeAngelis, G.C., Freeman, R.D., and Ohzawa, I. (1994). Length and width tuning of neurons in the cat's primary visual cortex. J. Neurophysiol. 71, 347–374.

DeAngelis, G.C., Ghose, G.M., Ohzawa, I., and Freeman, R.D. (1999). Functional micro-organization of primary visual cortex: receptive field analysis of nearby neurons. J. Neurosci. 19, 4046–4064.

Gilbert, C.D. (1977). Laminar differences in receptive field properties of cells in cat primary visual cortex. J. Physiol. 268, 391–421.

Gilbert, C.D. (1992). Horizontal integration and cortical dynamics. Neuron 9, 1–13.

Gilbert, C.D. (1998). Adult cortical dynamics. Physiol. Rev. 78, 467–485.

Gilbert, C.D., and Wiesel, T.N. (1990). The influence of contextual stimuli on the orientation selectivity of cells in primary visual cortex of the cat. Vision Res. 30, 1689–1701.

Gulyas, B., Orban, G.A., Duysens, J., and Maes, H. (1987). The suppressive influence of moving textured backgrounds on responses of cat striate neurons to moving bars. J. Neurophysiol. 57, 1767–1791.

Hubel, D.H., and Wiesel, T.N. (1977). Ferrier lecture. Functional architecture of macaque monkey visual cortex. Proc. R. Soc. Lond. B Biol. Sci. 198, 1–59.

Jones, H.E., Grieve, K.L., Wang, W., and Sillito, A.M. (2001). Surround suppression in primate V1. J. Neurophysiol. 86, 2011–2028.

Kapadia, M.K., Westheimer, G., and Gilbert, C.D. (1999). Dynamics of spatial summation in primary visual cortex of alert monkeys. Proc. Natl. Acad. Sci. USA 96, 12073–12078.

LeVay, S., and Voigt, T. (1988). Ocular dominance and disparity coding in cat visual cortex. Vis. Neurosci. 1, 395–414.

Levitt, J.B., and Lund, J.S. (1997). Contrast dependence of contextual effects in primate visual cortex. Nature 387, 73–76.

Li, C.Y. (1996). Integration fields beyond the classical receptive field: organization and functional properties. News Physiol. Sci. 11, 181–186.

Li, C.Y., and Li, W. (1994). Extensive integration field beyond the classical receptive field of cat's striate cortical neurons: classification and tuning properties. Vision Res. 34, 2337–2355.

Li, C.Y., Xu, X.Z., and Tigwell, D. (1995). A simple and comprehensive method for the construction, repair and recycling of single and double tungsten microelectrodes. J. Neurosci. Methods 57, 217–220.

Li, C.Y., Lei, J.J., and Yao, H.S. (1999). Shift in speed selectivity of visual cortex neurons: a neural basis of perceived motion contrast. Proc. Natl. Acad. Sci. USA 96, 4052–4056.

Lund, J.S., Henry, G.H., MacQueen, C.L., and Harvey, A.R. (1979). Anatomical organization of primary visual cortex (area 17) of the cat. A comparison with area 17 of the macaque monkey. J. Comp. Neurol. 184, 599–618.

Maffei, L., and Fiorentini, A. (1976). Monocular deprivation in kittens impairs the spatial resolution of geniculate neurones. Nature 264, 754–755.

Malach, R., Amir, Y., Harel, M., and Grinvald, A. (1993). Relationship between intrinsic connections and functional architecture revealed by optical imaging and in vivo targeted biocytin injections in primate striate cortex. Proc. Natl. Acad. Sci. USA 90, 10469–10473.

McGuire, B.A., Gilbert, C.D., Rivlin, P.K., and Wiesel, T.N. (1991). Targets of horizontal connections in macaque primary visual cortex. J. Comp. Neurol. 305, 370–392.

Nelson, J.I., and Frost, B.J. (1978). Orientation-selective inhibition from beyond the classic visual receptive field. Brain Res. 139, 359–365.

Payne, B.R., Berman, N., and Murphy, E.H. (1981). Organization of direction preferences in cat visual cortex. Brain Res. 211, 445–450.

Polat, U., Mizobe, K., Pettet, M.W., Kasamatsu, T., and Norcia, A.M. (1998). Collinear stimuli regulate visual responses depending on cell's contrast threshold. Nature 391, 580–584.

Rockland, K.S., and Lund, J.S. (1983). Intrinsic laminar lattice connections in primate visual cortex. J. Comp. Neurol. 216, 303–318.

Rossi, A.F., Desimone, R., and Ungerleider, L.G. (2001). Contextual modulation in primary visual cortex of macaques. J. Neurosci. 21, 1698–1709.

Sceniak, M.P., Ringach, D.L., Hawken, M.J., and Shapley, R. (1999). Contrast's effect on spatial summation by macaque V1 neurons. Nat. Neurosci. 2, 733–739.

Sengpiel, F., Sen, A., and Blakemore, C. (1997). Characteristics of surround inhibition in cat area 17. Exp. Brain Res. 116, 216–228.

Shmuel, A., and Grinvald, A. (1996). Functional organization for direction of motion and its relationship to orientation maps in cat area 18. J. Neurosci. 16, 6945–6964.

Shoham, D., Hubener, M., Schulze, S., Grinvald, A., and Bonhoeffer, T. (1997). Spatio-temporal frequency domains and their relation to cytochrome oxidase staining in cat visual cortex. Nature 385, 529–533.

Swindale, N.V., Shoham, D., Grinvald, A., Bonhoeffer, T., and Hubener, M. (2000). Visual cortex maps are optimized for uniform coverage. Nat. Neurosci. 3, 822–826.

Tolhurst, D.J., and Thompson, I.D. (1981). On the variety of spatial frequency selectivities shown by neurons in area 17 of the cat. Proc. R. Soc. Lond. B Biol. Sci. 213, 183–199.

Tootell, R.B., Silverman, M.S., and De Valois, R.L. (1981). Spatial frequency columns in primary visual cortex. Science 214, 813–815.

Tootell, R.B., Hamilton, S.L., and Switkes, E. (1988). Functional anatomy of macaque striate cortex. IV. Contrast and magno-parvo streams. J. Neurosci. 8, 1594–1609.

Walker, G.A., Ohzawa, I., and Freeman, R.D. (2000). Suppression outside the classical cortical receptive field. Vis. Neurosci. 17, 369–379.

Weliky, M., Bosking, W.H., and Fitzpatrick, D. (1996). A systematic map of direction preference in primary visual cortex. Nature 379, 725–728.